

# Identification of Hot Regions of the A $\beta$ –IAPP Interaction Interface as High-Affinity Binding Sites in both Cross- and Self-Association\*\*

Erika Andreetto, Li-Mei Yan, Marianna Tatarek-Nossol, Aleksandra Velkova, Ronald Frank, and Aphrodite Kapurniotu\*

Protein aggregation into cytotoxic aggregates and amyloid fibrils is associated with cell degeneration and the pathogenesis of numerous incurable diseases, including Alzheimer's disease (AD) and type 2 diabetes (T2D).<sup>[1,2]</sup> The 40- and 42-residue  $\beta$ -amyloid peptides A $\beta$ 40 and A $\beta$ 42 and the 37-residue islet amyloid polypeptide (IAPP) are key amyloid polypeptides in AD and in T2D, respectively.<sup>[1,2]</sup>

Emerging evidence supports the suggestion that, in addition to the self-interactions mediating pathogenic self-association, cross-amyloid interactions may also play a critical role in protein aggregation.<sup>[3–11]</sup> Examples of such interactions include the A $\beta$ –tau, the A $\beta$ – $\alpha$ -synuclein, the A $\beta$ –transthyretin, and the IAPP–insulin interaction.<sup>[7,9,11,12]</sup> A recently uncovered cross-amyloid interaction is the A $\beta$ 40–IAPP interaction (Figure 1).<sup>[3]</sup> This low-nanomolar-affinity interaction between early nonfibrillar and nontoxic A $\beta$ 40 and

IAPP species, which was identified *in vitro*, has been shown to suppress cytotoxic self-association and amyloidogenesis by both A $\beta$ 40 and IAPP.<sup>[3]</sup> These results have led to the hypothesis that the A $\beta$ 40–IAPP hetero-association might be a molecular link between AD and T2D, which is consistent with clinical and epidemiological evidence linking the two diseases.<sup>[13,14]</sup> As A $\beta$  and IAPP are present in serum and cerebrospinal fluid at similar concentrations, an *in-vivo* interaction might be possible. In fact, very recent immunohistochemical studies showed that A $\beta$  co-localizes with IAPP in pancreatic islet amyloid aggregates of T2D patients.<sup>[15]</sup> Understanding the molecular determinants of the A $\beta$ –IAPP hetero- versus self-association is thus of high biomedical importance in shedding light into both their links to disease pathogenesis and in designing compounds to modulate these processes.

A $\beta$  and IAPP are intrinsically disordered but highly amyloidogenic polypeptides.<sup>[16,17]</sup> These peptides have a circa 25% degree of shared sequence identity and about 50% similarity with highest degrees of identity and similarity being observed between sequences of critical importance for amyloid self-assembly of both A $\beta$  and IAPP (overlapping yellow and pink areas in Figure 1).<sup>[6,18–22]</sup> Herein we present a systematic study of the cross- and self-interaction interface of A $\beta$  and IAPP. We identify short A $\beta$  and IAPP peptide sequences as hot regions of the A $\beta$ –IAPP cross-interaction interface; that is, as the shortest sequences that are able to cross-interact with IAPP or A $\beta$  with affinities in the nano- to low micromolar range. Moreover, the identified peptides are shown to be high affinity ligands of both A $\beta$  and IAPP suggesting common molecular recognition features in amyloid self- and cross-amyloid hetero-assembly.

We first addressed the question as to what regions of A $\beta$ 40 bind IAPP by using membrane-bound peptide arrays of 10-residue A $\beta$ 40 sequences covering full-length A $\beta$ 40 and positionally shifted by one residue (Figure 2).<sup>[24]</sup> Membranes were incubated with synthetic N<sup>α</sup>-amino-terminal biotin-labeled IAPP–GI (biotin–IAPP–GI).<sup>[25]</sup> Of note, the double N-methylated IAPP mimic [(N-Me)G24, (N-Me)I26]–IAPP (IAPP–GI) was applied as a substitute for the highly insoluble and aggregation-prone IAPP owing to its excellent solubility and non-amyloidogenic character.<sup>[25]</sup> In fact, IAPP–GI has been shown to bind A $\beta$ 40 with the same affinity as non-aggregated IAPP.<sup>[3]</sup> A $\beta$ 40 decamers that bound biotin–IAPP–GI were identified by incubation with streptavidin-conjugated peroxidase (POD) (Figure 2). Two clusters of 3–4 consecutive sequences were identified: the first in A $\beta$ (12–24) and the second one in A $\beta$ (26–37).



**Figure 1.** Primary structures of A $\beta$  and IAPP. Identical residues between sequences are indicated in blue and similar residues in green.<sup>[3,10]</sup> The shortest sequences with highest degrees of identity and similarity are underlined in yellow. Domains previously suggested to be involved in self-association are underlined in pink.<sup>[6,18–23]</sup>

[\*] E. Andreetto, Dr. L.-M. Yan, Dr. A. Velkova, Prof. Dr. A. Kapurniotu  
Laboratory of Peptide Biochemistry  
Center of Integrated Protein Science  
Technische Universität München, Emil-Erlenmeyer-Forum 5  
85354 Freising-Weihenstephan (Germany)  
Fax: (+49) 8161-713-298  
E-mail: akapurniotu@wzw.tum.de  
Homepage: <http://www.wzw.tum.de/pbch>  
M. Tatarek-Nossol  
Lehrstuhl für Biochemie und Molekulare Zellbiologie  
RWTH Aachen  
52074 Aachen (Germany)  
Dr. R. Frank  
Abteilung Chemische Biologie  
Helmholtz Zentrum für Infektionsforschung  
38106 Braunschweig (Germany)

[\*\*] E. Andreetto and L.-M. Yan contributed equally to this work. This work has been supported by the Deutsche Forschungsgemeinschaft (DFG). We are grateful to S. Daenicke for synthesis of peptide arrays.

Supporting information for this article is available on the WWW under <http://dx.doi.org/10.1002/anie.200904902>.

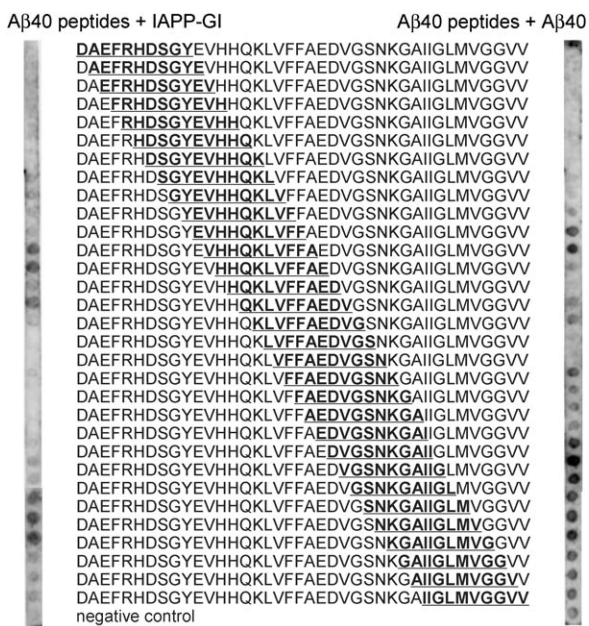


**Figure 2.** Identification of A $\beta$ 40 regions that bind IAPP (IAPP-GI) (left) or A $\beta$ 40 (right). The A $\beta$ 40 decamers shown in bold and underlined were incubated with biotin-IAPP-GI (left) or biotin-A $\beta$ 40 (right). Bound biotin-IAPP-GI or biotin-A $\beta$ 40 were detected following incubation with streptavidin-POD and development by ECL. Membranes represent 2–3 assays.

The identified IAPP binding A $\beta$ 40 segments comprise sequences that are major parts of the  $\beta$  strands of A $\beta$ 40 amyloid (pink in Figure 1).<sup>[19,26–28]</sup> Our results thus indicate that A $\beta$ 40 regions involved in hetero-association with IAPP might also be involved in A $\beta$ 40 self-association. To test this hypothesis, membranes containing A $\beta$ 40 decamers were incubated with synthetic N<sup>q</sup>-amino terminal biotinylated A $\beta$ 40 (biotin-A $\beta$ 40) and sequences that bound biotin-A $\beta$ 40 were revealed after incubation with streptavidin-POD (Figure 2). In fact, A $\beta$ 40 regions that bound biotin-A $\beta$ 40 were localized within A $\beta$ (11–21) and A $\beta$ (23–37), which are very similar regions to those involved in hetero-association (Figure 2).

To identify the IAPP regions that interact with A $\beta$ 40, we applied membrane-bound peptide arrays with 10-residue IAPP peptide sequences covering full-length IAPP and positionally shifted by one residue (Figure 3). Following incubation with A $\beta$ 40, A $\beta$ 40 binding sequences were revealed with anti-A $\beta$ 40 antibody. All peptides within the N-terminal region IAPP(1–20) bound A $\beta$ 40 (Figure 3). As weak A $\beta$ 40 binding was also observed in some of the sequences within IAPP(21–37), and to exclude the possibility that the high hydrophobicity and self-association propensity of these membrane-bound peptides might have hindered their binding to A $\beta$ 40, a membrane containing twelve non-amyloidogenic decapeptides N-methylated at G24 and I26 and spanning IAPP-GI(15–35) was also tested. In fact, most of these peptides bound A $\beta$ 40 (Figure 3). These results were consistent with two A $\beta$ 40 binding sites in IAPP, the first being localized within IAPP(8–20) and the second within IAPP(23–35).

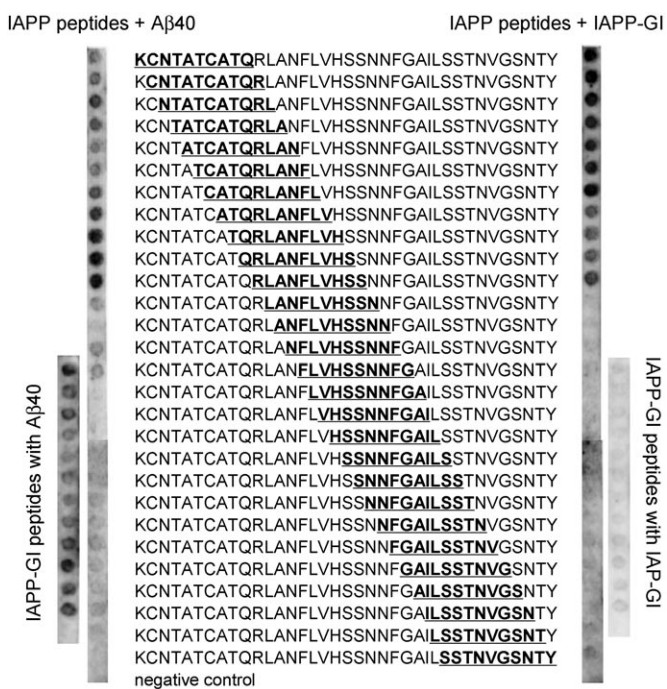


**Figure 3.** Identification of IAPP regions that bind A $\beta$ 40 (left membrane) or IAPP (IAPP-GI) (right membrane) using peptide arrays. Decamers corresponding to overlapping IAPP sequences (bold and underlined) were incubated with A $\beta$ 40 (left) or biotin-IAPP-GI (right). Bound A $\beta$ 40 or biotin-IAPP-GI were detected following incubation with anti-A $\beta$ 40 or streptavidin-POD and ECL. Membranes at the lower left or right sides consist of the decamers spanning IAPP-GI(15–35) which were also probed for binding to A $\beta$ 40 (lower left) or to IAPP-GI (lower right), as above. Membranes are representative from 2–3 assays.

The identified IAPP regions that bound A $\beta$ 40 contained sequences suggested to mediate IAPP self-association into amyloid fibrils.<sup>[6,18,20-22,29]</sup> We therefore probed binding of the IAPP peptide membrane with biotin-IAPP-GI. In fact, all strong biotin-IAPP binders localized within IAPP(1-20) while a weaker interaction was observed for sequences within the C-terminal IAPP part (Figure 3).<sup>[21]</sup> Thus, IAPP regions which are important for its hetero-association with A $\beta$ 40 appear to mediate its self-association as well.

To confirm the above results and to characterize the interaction interface of A $\beta$ 40 and IAPP more precisely, a number of partial A $\beta$ 40 and IAPP sequences and their fluorescently labeled analogues were synthesized, and their interactions with IAPP and A $\beta$ 40 were characterized by fluorescence titration binding assays (Tables 1 and 2).<sup>[3,25]</sup> To determine the A $\beta$ 40 sequences that bind IAPP, N<sup>α</sup>-amino-terminal fluorescein-labeled IAPP (Fluos-IAPP) was first titrated with the two major A $\beta$ 40 segments, A $\beta$ (1–28) and A $\beta$ (29–40), corresponding to the extracellular hydrophilic and the transmembrane hydrophobic A $\beta$ 40 parts; each of these parts contribute one strand to the  $\beta$  sheet of A $\beta$ 40 amyloid (Figure 1).<sup>[19]</sup> Both segments bound IAPP, with A $\beta$ (29–40) being the stronger ligand ( $K_{d,app}$ =200 nM) and A $\beta$ (1–28) the weaker ( $K_{d,app}$ =2.5  $\mu$ M; Table 1). These results

**Table 1:** Identification of A $\beta$ 40 hot regions (in bold) that bind full-length IAPP and A $\beta$ 40 and determination of apparent binding affinities ( $K_{d,app}$ ) by fluorescence titration binding assays.<sup>[a]</sup>

A $\beta$ 40 sequence	$K_{d,app}$ (for IAPP) <sup>[b,c]</sup>	$K_{d,app}$ (for A $\beta$ 40) <sup>[b,c]</sup>
A $\beta$ 40	48.5 nM ( $\pm$ 4.2) <sup>[3]</sup>	198 nM ( $\pm$ 43)
A $\beta$ (1–28)	2.5 $\mu$ M	711 nM
A $\beta$ (12–28)	2.8 $\mu$ M	n.d.
A $\beta$ (15–24)	6.4 $\mu$ M ( $\pm$ 1.0)	1.0 $\mu$ M ( $\pm$ 0.1)
A $\beta$ (15–21)	14.0 $\mu$ M	2.9 $\mu$ M
A $\beta$ (16–21)	13.8 $\mu$ M	n.d.
A $\beta$ (18–21)	2.1 $\mu$ M	–
A $\beta$ (19–21)	–	n.d.
<b>A<math>\beta</math>(19–22)</b>	<b>7.0 <math>\mu</math>M (<math>\pm</math> 0.7)</b>	<b>5.5 <math>\mu</math>M (<math>\pm</math> 0.6)</b>
A $\beta$ (29–40)	200 nM	463 nM
A $\beta$ (25–35)	282 nM ( $\pm$ 29)	326 nM ( $\pm$ 61)
<b>A<math>\beta</math>(27–32)</b>	<b>477 nM (<math>\pm</math> 114)<sup>[d]</sup></b>	<b>282 nM (<math>\pm</math> 47)</b>
A $\beta$ (28–32)	–	–
A $\beta$ (27–31)	–	–
<b>A<math>\beta</math>(35–40)</b>	<b>354 nM (<math>\pm</math> 36)</b>	<b>358 nM (<math>\pm</math> 25)</b>
A $\beta$ (35–39)	3.1 $\mu$ M	4.1 $\mu$ M
A $\beta$ (35–38)	–	–
A $\beta$ (36–40)	–	28.6 $\mu$ M

[a] Titrations were performed in 10 mM sodium phosphate buffer, pH 7.4, containing 1% HFIP. N<sup>α</sup>-amino-terminal fluorescently labeled IAPP or A $\beta$ 40 were titrated with A $\beta$ 40 segments.<sup>[3,25]</sup> [b]  $K_{d,app}$  values were determined from one or three binding curves; numbers in parentheses indicate the standard error ( $\pm$ ) from three binding curves. [c] – no binding at concentrations  $\leq$  20  $\mu$ M; n.d. = not determined. [d]  $K_{d,app}$  of A $\beta$ (27–32)–IAPP–GI interaction.

suggested that the hydrophobic C-terminal part A $\beta$ (29–40) plays a crucial role in the A $\beta$ 40–IAPP interaction.<sup>[3]</sup>

To identify the shortest A $\beta$ 40 sequences that are still able to bind IAPP, peptides devised by systematic shortening of A $\beta$ (1–28) and A $\beta$ (29–40) at both the C-terminal and the N-terminal ends or based on structural models of A $\beta$ 40 were then synthesized and tested for binding to IAPP (Table 1; Supporting Information, Figure S1).<sup>[19,28,30]</sup> Of note, very similar affinities were obtained when IAPP–GI was used instead of IAPP (data not shown). A $\beta$ (27–32) (NKGAI) and A $\beta$ (35–40) (MVGGVV) were identified as the shortest sequences that were able to bind IAPP with nanomolar affinity. Within A $\beta$ (1–28), the sequences A $\beta$ (18–21) (VFFA) and A $\beta$ (19–22) (FFAE) were the shortest that bound IAPP. The affinities of their interactions with IAPP were in the low  $\mu$ M range, similar to the A $\beta$ (1–28)–IAPP interaction.

The interactions of the identified IAPP binding A $\beta$ 40 sequences with A $\beta$ 40 were then studied (Table 1; Supporting Information, Figure S1). Both A $\beta$ (27–32) and A $\beta$ (35–40) bound A $\beta$ 40 with  $K_{d,app}$  values that were nearly identical to the  $K_{d,app}$  values of their interaction with IAPP. Peptides shorter than A $\beta$ (27–32) or A $\beta$ (35–40) did not bind or only weakly bound A $\beta$ 40. Finally, A $\beta$ (19–22) proved to be the shortest sequence within A $\beta$ (1–28), which bound both IAPP and A $\beta$ , albeit with low  $\mu$ M affinities. The results of the fluorescence titration assays were consistent with the results of the peptide arrays and, furthermore, they identified the two hexapeptides A $\beta$ (27–32) and A $\beta$ (35–40) and the tetrapeptide A $\beta$ (19–22) as the shortest A $\beta$ 40 sequences that bind both IAPP and A $\beta$ 40 with nanomolar or low-micromolar affinities

(Table 1). The results of both assays are summarized in Figure 4.

To identify the shortest IAPP sequences which bind A $\beta$ 40, IAPP was first dissected in IAPP(1–18) and IAPP(19–37),

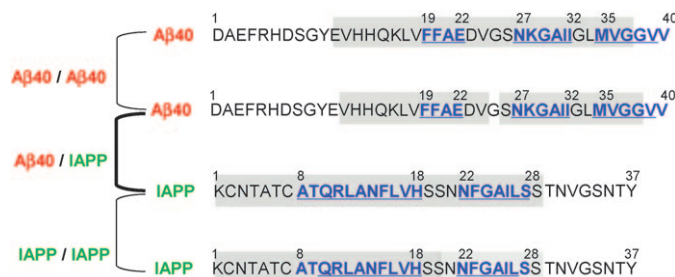


**Figure 4.** Cross- and self-interacting domains of A $\beta$ 40 and IAPP as indicated by binding studies with peptide arrays (gray bars; light gray: weak interaction) and hot regions (blue letters) of the A $\beta$ 40–IAPP, A $\beta$ 40–A $\beta$ 40, and IAPP–IAPP interaction interfaces as determined by fluorescence titration binding assays. Underlined sequences indicate the shortest peptide segments that are still able to bind A $\beta$ 40 and IAPP, albeit with weaker affinities than the hot regions.

and their interactions with A $\beta$ 40 were studied.<sup>[17]</sup> IAPP(1–18) is the N-terminal, less-amyloidogenic IAPP part that contains the short amyloidogenic segment IAPP(14–18).<sup>[21]</sup> IAPP(19–37) is the hydrophobic and strongly amyloidogenic C-terminal part containing the amyloidogenic sequences IAPP(22–27) and IAPP(30–37).<sup>[20,31]</sup> Both IAPP(1–18) and IAPP(19–37) bound A $\beta$ 40 with nanomolar affinities (Table 2, Supporting Information, Figure S2). Systematic sequence shortening and fluorescence binding assays followed. IAPP(8–18) and IAPP(22–28) were identified as the shortest sequences that are still able to bind A $\beta$ 40 with affinities in the nanomolar range (Table 2; Supporting Information, Figure S2). Of note, IAPP(10–18) was found to be the shortest recognition element within IAPP(1–18) necessary for the A $\beta$ 40–IAPP interaction, but it bound A $\beta$ 40 with a significantly weaker affinity than IAPP(8–18). This result may be due to the fact that the A $\beta$ 40 hot region A $\beta$ (27–32) bound IAPP(8–18) but was unable to bind IAPP(10–18), as revealed by cross-interaction studies (Table 3).

Because IAPP(8–18) and IAPP(22–28) have been suggested to mediate IAPP self-assembly, our results indicated that the same IAPP regions might also be involved in its hetero-association pathways.<sup>[6,21,29]</sup> We therefore studied binding of the above IAPP sequences to IAPP (Table 2; Supporting Information, Figure 2). In fact, the binding affinities of all IAPP sequences to IAPP were very similar to their A $\beta$ 40 affinities. The results, summarized in Figure 4, suggest that IAPP(8–18) and IAPP(22–28) are hot regions of both the IAPP–A $\beta$ 40 and the IAPP–IAPP interaction interface.

To determine the binding site(s) of the identified hot regions within A $\beta$ 40 and IAPP, we then studied cross-interactions between them or slightly elongated sequences by using fluorescence titration assays (Table 3; Supporting Information, Tables S1, S2). As summarized in Figure 5, a broad network of nanomolar to low-micromolar self- and



**Table 2:** Identification of IAPP hot regions (in bold) that bind full-length Aβ40 or IAPP and determination of  $K_{d,app}$  by fluorescence titration assays.<sup>[a]</sup>

IAPP sequences	$K_{d,app}$ (for Aβ40) <sup>[b,c]</sup>	$K_{d,app}$ (for IAPP) <sup>[b,c]</sup>
IAPP	48.5 nM ( $\pm 4.2$ ) <sup>[3]</sup>	9.7 ( $\pm 0.9$ ) <sup>[25]</sup>
IAPP(1-18)	183 nM ( $\pm 56$ )	125 nM ( $\pm 18$ )
<b>IAPP(8-18)</b>	<b>275 nM (<math>\pm 28</math>)</b>	<b>233 nM (<math>\pm 59</math>)</b>
IAPP(9-18)	1.0 $\mu$ M ( $\pm 0.1$ )	535 nM ( $\pm 6$ )
IAPP(10-18)	1.3 $\mu$ M ( $\pm 0.1$ )	569 nM ( $\pm 12$ )
IAPP(11-18)	–	–
IAPP(10-17)	–	–
IAPP(1-7)	–	–
IAPP(19-37)	281 nM ( $\pm 20$ )	374 nM ( $\pm 10$ )
IAPP(20-29)	322 nM ( $\pm 25$ )	293 nM ( $\pm 23$ )
IAPP(21-28)	587 nM	316 nM
<b>IAPP(22-28)</b>	<b>363 nM (<math>\pm 36</math>)</b>	<b>398 nM (<math>\pm 70</math>)</b>
IAPP(23-28)	–	795 nM
IAPP(24-28)	n.d.	–
IAPP(22-27)	–	1.2 $\mu$ M
IAPP(23-27)	n.d.	–
IAPP(22-26)	n.d.	–
IAPP(30-37)	–	–

[a] Titrations were performed in 10 mM sodium phosphate buffer, pH 7.4, containing 1% HFIP. N<sup>α</sup>-amino-terminal fluorescently labeled IAPP and IAPP segments were titrated with Aβ40 or IAPP.<sup>[3,25]</sup> [b]  $K_{d,app}$  values were determined from one or three binding curves; numbers in parentheses indicate the ( $\pm$ ) standard error from three binding curves. [c] – no binding at concentrations  $\leq 3 \mu$ M; n.d. = not determined.

**Table 3:**  $K_{d,app}$  values as determined by fluorescence titration assays for cross-interactions between the identified Aβ40-IAPP hot regions within Aβ40 and IAPP (in bold), or slightly elongated sequences thereof.<sup>[a,b]</sup>

Aβ40 sequence	$K_{d,app}$		
	with IAPP(8-18)	with IAPP(22-28)	with IAPP(20-29)
<b>Aβ(19-22)</b> <sup>[d]</sup>	2.9 $\mu$ M	– <sup>[e]</sup>	– <sup>[e]</sup>
Aβ(15-24) <sup>[d]</sup>	4.2 $\mu$ M	6.7 $\mu$ M	6.4 $\mu$ M
<b>Aβ(27-32)</b> <sup>[d]</sup>	1.4 $\mu$ M	566 nM <sup>[f]</sup>	305 nM
Aβ(25-35) <sup>[d]</sup>	902 nM	426 nM	698 nM
<b>Aβ(35-40)</b> <sup>[d]</sup>	1.1 $\mu$ M	– <sup>[e]</sup>	869 nM

[a] Titrations were performed in 10 mM sodium phosphate buffer, pH 7.4 containing 1% HFIP. [b]  $K_{d,app}$  values were determined from one binding curve. [c] N<sup>α</sup>-amino-terminal fluorescein-labeled Aβ40 segments were titrated with IAPP segments.<sup>[3,25]</sup> [d] N<sup>α</sup>-amino-terminal fluorescein-labeled IAPP segments were titrated with Aβ40 segments.<sup>[3,25]</sup> [e] – no binding was observed at peptide concentrations  $\leq 20 \mu$ M. [f]  $K_{d,app}$  values of the Aβ(27-32)–IAPP(21-28) interaction (no binding with IAPP(22-28)).

cross-interactions was found. These data suggest that strong cooperative interactions between the same binding sites are involved in both the hetero- and the self-association pathways of Aβ40 and IAPP. Of note, the validity of the results of our studies was confirmed by a number of control studies (Supporting Information, Figure S3).

The self-assembly process of Aβ42 is believed to play an utmost important role in AD pathogenesis.<sup>[32]</sup> Therefore, we also addressed the question whether Aβ42 interacts with IAPP and IAPP-GI in a similar manner as Aβ40.<sup>[3]</sup> In fact, our results suggested that Aβ42 interacts with IAPP and IAPP-GI in a similar manner as previously shown for Aβ40, that the

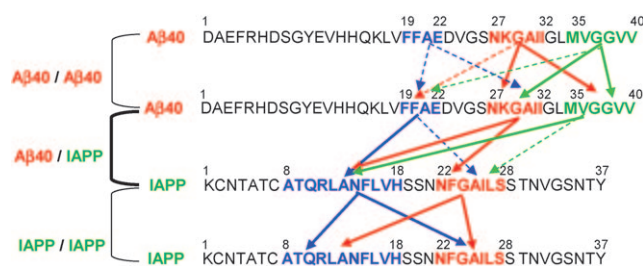


**Figure 5:** Summary of the determined cross- and self-interactions between the hot (solid arrows) or slightly longer sequences (dashed arrows) of the Aβ40-IAPP interaction interface (hot regions in blue, red, and green; see also Table 3 and the Supporting Information, Tables S1, S2). For interactions involving longer regions, the following sequences were used: Aβ(15-24) instead of Aβ(19-22), Aβ(25-35) instead of Aβ(27-32), and IAPP(20-29) instead of IAPP(22-28).

Aβ42–IAPP interaction suppresses cytotoxic oligomerization and amyloidogenesis by both polypeptides, and that this interaction is mediated by the same hot regions as the Aβ40–IAPP interaction (Supporting Information, Figures S4–S6 and Tables S3, S4).<sup>[3]</sup> Of note, the Aβ42–IAPP–GI interaction inhibited formation of cytotoxic species and amyloid fibrils by Aβ42, as recently shown for the Aβ40–IAPP–GI interaction (Supporting Information, Figures S4–S6).<sup>[3]</sup>

Taken together, our results provide evidence that hetero-association underlying high-affinity cross-amyloid interactions between Aβ and IAPP proceed by their amyloid self-recognition domains. Our results also suggest that hetero- and self-association of Aβ and IAPP most likely occur in a competitive manner by a flexible and broad network of high affinity, multiple, and cooperative intra- and intermolecular self- and cross-interactions between the identified hot regions. In fact, the high conformational flexibility of both Aβ and IAPP monomers would enable such interactions.<sup>[16]</sup> The identified broad cross-interaction network could account for the high affinities of the self- and the cross-interactions of Aβ and IAPP, and it would also allow for formation of polymorphic supramolecular structures including both hetero- and homo-assemblies. This interaction network is consistent with structural models of Aβ and IAPP amyloid fibrils and their polymorphism, although detailed structural information on the Aβ–IAPP hetero-assemblies is not yet available.<sup>[6, 18, 19, 22, 23, 33, 34]</sup>

Previous studies have identified short peptide sequences with high  $\beta$ -sheet-forming and amyloidogenic potentials.<sup>[20, 28, 30]</sup> Such sequences may confer amyloidogenicity to a polypeptide chain.<sup>[35]</sup> Our results, and recent results by others, support the hypothesis that, in addition to such amyloid motifs, cross-amyloid recognition patterns may also exist that may be very similar or identical to the amyloid ones.<sup>[5–7]</sup> In fact, the two segments IAPP(8-18) and IAPP(22-28), which mediate IAPP hetero-association with Aβ, also drive self-association of IAPP into amyloid fibrils. Furthermore, these two IAPP segments have been suggested to mediate IAPP binding to insulin,<sup>[5, 6, 21, 22, 29]</sup> while the IAPP-binding Aβ sequences identified herein, Aβ(27-32) and Aβ(35-40(42)), have been shown to be core regions of the Aβ–tau interaction as well.<sup>[7]</sup>

In conclusion, our studies identify five short peptide segments of A $\beta$  and IAPP as hot regions of the A $\beta$ –IAPP cross-interaction interface and show that these peptides are able to self- and to cross-interact and that they are high-affinity ligands of both A $\beta$  and IAPP. Our results suggest that molecular recognition features underlying amyloid self-assembly of A $\beta$ , IAPP, and most likely other amyloidogenic polypeptides also mediate cross-amyloid hetero-assembly. Our results offer thus a novel molecular basis for understanding interactions involved in amyloidogenic and cytotoxic protein self-assembly in AD and T2D and possibly other protein aggregation diseases and should assist in designing compounds to block these processes.

Received: September 1, 2009

Revised: December 25, 2009

Published online: March 22, 2010

**Keywords:**  $\beta$ -amyloid peptides · islet amyloid polypeptides · molecular recognition · protein interactions · protein self-assembly

- [1] F. Chiti, C. M. Dobson, *Annu. Rev. Biochem.* **2006**, *75*, 333–366.
- [2] P. Westermark, *FEBS J.* **2005**, *272*, 5942–5949.
- [3] L. M. Yan, A. Velkova, M. Taterek-Nossol, E. Andreetto, A. Kapurniotu, *Angew. Chem.* **2007**, *119*, 1268–1274; *Angew. Chem. Int. Ed.* **2007**, *46*, 1246–1252.
- [4] A. Velkova, M. Taterek-Nossol, E. Andreetto, A. Kapurniotu, *Angew. Chem.* **2008**, *120*, 7222–7227; *Angew. Chem. Int. Ed.* **2008**, *47*, 7114–7118.
- [5] S. Gilead, H. Wolfenson, E. Gazit, *Angew. Chem.* **2006**, *118*, 6626–6630; *Angew. Chem. Int. Ed.* **2006**, *45*, 6476–6480.
- [6] J. J. Wiltzius, S. A. Sievers, M. R. Sawaya, D. Eisenberg, *Protein Sci.* **2009**, *18*, 1521–1530.
- [7] J. P. Guo, T. Arai, J. Miklossy, P. L. McGeer, *Proc. Natl. Acad. Sci. USA* **2006**, *103*, 1953–1958.
- [8] J. Laurén, D. A. Gimbel, H. B. Nygaard, J. W. Gilbert, S. M. Strittmatter, *Nature* **2009**, *457*, 1128–1132.
- [9] P. Westermark, Z.-C. Li, G. Westermark, A. Leckström, D. Steiner, *FEBS Lett.* **1996**, *379*, 203–206.
- [10] B. O’Nuallain, A. D. Williams, P. Westermark, R. Wetzel, *J. Biol. Chem.* **2004**, *279*, 17490–17499.
- [11] B. I. Giasson, M. S. Forman, M. Higuchi, L. I. Golbe, C. L. Graves, P. T. Kotzbauer, J. Q. Trojanowski, V. M. Lee, *Science* **2003**, *300*, 636–640.
- [12] J. N. Buxbaum, Z. Ye, N. Reixach, L. Friske, C. Levy, P. Das, T. Golde, E. Masliah, A. R. Roberts, T. Bartfai, *Proc. Natl. Acad. Sci. USA* **2008**, *105*, 2681–2686.
- [13] M. R. Nicolls, *Curr. Alzheimer Res.* **2004**, *1*, 47–54.
- [14] L. Li, C. Hölscher, *Brain Res. Rev.* **2007**, *56*, 384–402.
- [15] J. Miklossy, H. Qing, A. Radenovic, A. Kis, B. Vilen, F. Laszlo, L. Miller, R. N. Martins, G. Waeber, V. Mooser, F. Bosman, K. Khalili, N. Darbinian, P. L. McGeer, *Neurobiol. Aging* **2008**, *29*, DOI: 10.1016/j.neurobiolaging.2008.08.019.
- [16] V. N. Uversky, A. L. Fink, *Biochim. Biophys. Acta Proteins Proteomics* **2004**, *1698*, 131–153.
- [17] A. Kapurniotu, *Biopolymers* **2001**, *60*, 438–459.
- [18] S. Luca, W. M. Yau, R. Leapman, R. Tycko, *Biochemistry* **2007**, *46*, 13505–13522.
- [19] A. T. Petkova, Y. Ishii, J. J. Balbach, O. N. Antzutkin, R. D. Leapman, F. Delaglio, R. Tycko, *Proc. Natl. Acad. Sci. USA* **2002**, *99*, 16742–16747.
- [20] K. Tenidis, M. Waldner, J. Bernhagen, W. Fischle, M. Bergmann, M. Weber, M.-L. Merkle, W. Voelter, H. Brunner, A. Kapurniotu, *J. Mol. Biol.* **2000**, *295*, 1055–1071.
- [21] Y. Mazar, S. Gilead, I. Benhar, E. Gazit, *J. Mol. Biol.* **2002**, *322*, 1013–1024.
- [22] S. H. Shim, R. Gupta, Y. L. Ling, D. B. Strasfeld, D. P. Raleigh, M. T. Zanni, *Proc. Natl. Acad. Sci. USA* **2009**, *106*, 6614–6619.
- [23] T. Luhrs, C. Ritter, M. Adrian, D. Riek-Loher, B. Bohrmann, H. Dobeli, D. Schubert, R. Riek, *Proc. Natl. Acad. Sci. USA* **2005**, *102*, 17342–17347.
- [24] R. Frank, *Tetrahedron* **1992**, *48*, 9217–9232.
- [25] L. M. Yan, M. Taterek-Nossol, A. Velkova, A. Kazantzis, A. Kapurniotu, *Proc. Natl. Acad. Sci. USA* **2006**, *103*, 2046–2051.
- [26] R. Wetzel, S. Shivaprasad, A. D. Williams, *Biochemistry* **2007**, *46*, 1–10.
- [27] L. O. Tjernberg, J. Näslund, F. Lindquist, J. Johanson, A. Karlström, J. Thyberg, J. Terenius, C. Nordstedt, *J. Biol. Chem.* **1996**, *271*, 8545–8548.
- [28] M. Lopez de La Paz, L. Serrano, *Proc. Natl. Acad. Sci. USA* **2004**, *101*, 87–92.
- [29] R. Mishra, M. Geyer, R. Winter, *ChemBioChem* **2009**, *10*, 1769–1772.
- [30] M. R. Sawaya, S. Sambashivan, R. Nelson, M. I. Ivanova, S. A. Sievers, M. I. Apostol, M. J. Thompson, M. Balbirnie, J. J. Wiltzius, H. T. McFarlane, A. O. Madsen, C. Riek, D. Eisenberg, *Nature* **2007**, *447*, 453–457.
- [31] M. R. Nilsson, D. P. Raleigh, *J. Mol. Biol.* **1999**, *294*, 1375–1385.
- [32] M. A. Findeis, *Pharmacol. Ther.* **2007**, *116*, 266–286.
- [33] C. S. Goldsbury, G. J. S. Cooper, K. N. Goldie, S. A. Müller, E. L. Saafi, W. T. M. Gruijters, M. P. Misur, A. Engel, U. Aebi, J. Kistler, *J. Struct. Biol.* **1997**, *119*, 12–27.
- [34] A. K. Paravastu, R. D. Leapman, W.-M. Yau, R. Tycko, *Proc. Natl. Acad. Sci. USA* **2008**, *105*, 18349–18354.
- [35] A. Esteras-Chopo, L. Serrano, M. Lopez de La Paz, *Proc. Natl. Acad. Sci. USA* **2005**, *102*, 16672–16677.